

This is an Open Access document downloaded from ORCA, Cardiff University's institutional repository: <https://orca.cardiff.ac.uk/id/eprint/109195/>

This is the author's version of a work that was submitted to / accepted for publication.

Citation for final published version:

Hosking, L. J. . , Thomas, H. R. and Sedighi, M. 2018. A dual porosity model of high pressure gas flow for geoenery applications. Canadian Geotechnical Journal 55 (6) , pp. 839-851. 10.1139/cgj-2016-0532

Publishers page: <http://dx.doi.org/10.1139/cgj-2016-0532>

Please note:

Changes made as a result of publishing processes such as copy-editing, formatting and page numbers may not be reflected in this version. For the definitive version of this publication, please refer to the published source. You are advised to consult the publisher's version if you wish to cite this paper.

This version is being made available in accordance with publisher policies. See <http://orca.cf.ac.uk/policies.html> for usage policies. Copyright and moral rights for publications made available in ORCA are retained by the copyright holders.



A dual porosity model of high pressure gas flow for geoenergy applications

Hosking, L.J.¹, Thomas, H.R.¹, and Sedighi, M.²

¹*Geoenvironmental Research Centre, Cardiff School of Engineering, Cardiff University, The Queen's Buildings, Newport Road, Cardiff, CF24 3AA, UK*

²*School of Mechanical, Aerospace and Civil Engineering, The University of Manchester, Manchester, M1 3PL, UK*

Abstract

This paper presents the development of a dual porosity numerical model of multiphase, multicomponent chemical/gas transport using a coupled thermal, hydraulic, chemical and mechanical formulation. Appropriate relationships are used to describe the transport properties of non-ideal, reactive gas mixtures at high pressure, enabling the study of geoenergy applications such as geological carbon sequestration. Theoretical descriptions of the key transport processes are based on a dual porosity approach considering the fracture network and porous matrix as distinct continua over the domain. Flow between the pore regions is handled using mass exchange terms and the model includes equilibrium and kinetically-controlled chemical reactions. A numerical solution is obtained with a finite element and finite difference approach and verification of the model is pursued to build confidence in the accuracy of the implementation of the dual porosity governing equations. In the course of these tests, the time splitting approach used to couple the transport, mass exchange and chemical reaction modules is shown to have been successfully applied. It is claimed that the modelling platform developed provides an advanced tool for the study of high pressure gas transport, storage and displacement for geoenergy applications involving multiphase, multicomponent chemical/gas transport in dual porosity media, such as geological carbon sequestration.

Keywords: dual porosity, gas flow, high pressure, carbon sequestration, geoenergy

¹ Corresponding author: Dr Lee J. Hosking
Geoenvironmental Research Centre, Cardiff School of Engineering, Cardiff University, Queen's Buildings, The Parade, CF24 3AA, Cardiff, UK, Email: HoskingL@cardiff.ac.uk, Tel: 02920 870497

Introduction

Climate change poses a great threat to the environment and society, yet there is a growing global demand for energy and energy security is a political priority. Geoenergy technologies are prominent in the strategies for climate change mitigation and adaptation developed as a collective response to these issues. Geological carbon sequestration, for example, is intended to facilitate the decarbonisation of reliable fossil fuel power plants by isolating carbon dioxide emissions in suitable deep rock formations (Scott, Gilfillan et al. 2013). Other examples include enhanced hydrocarbon recovery, the exploration of unconventional gas, and the deep geological disposal of nuclear waste. It is therefore important from an engineering perspective to examine the complex, coupled phenomena governing the transport, storage and displacement of multiphase, multicomponent chemicals and gas in the deep geoenvironment. This study addresses the development of a numerical model for this purpose.

Fractures and discontinuities are commonly important features in geological formations and can have a significant bearing on the water and gas flows and reactive chemical transport. They effectively divide a geomaterial into two distinct porosities, namely, the fracture network and the porous matrix blocks (Bear 1993). An understanding of the physical and chemical processes involved in multiphase flow in each of these pore regions is important for a rigorous prediction of the phenomena arising in the geoenergy applications mentioned above. Of particular interest are the differences in the fluid transport and displacement behaviour, which may depend strongly on the inter-porosity flows and various physical and chemical interactions between the solid, liquid and gas phases.

Several established modelling techniques are available to express the heterogeneous pore structure of a dual porosity geomaterial in a form more amenable to numerical treatment. In broad terms, these may be categorised as: i) discrete fracture network (DFN) models, ii) equivalent continuum models, and iii) dual (or higher) porosity models (Therrien and Sudicky 1996). The selection of the most appropriate type of model depends on the problem scale/conditions, the available input data, the type of output data required, and the available computational resources (Bear 1993, Samardzioska and Popov 2005).

DFN models can provide a theoretically rigorous interpretation of a fractured rock, since an attempt is made to explicitly model the flow in each and every hydraulically active fracture. They are attractive

provided these fractures can be identified and included within the modelling framework without excessive costs in terms of input data and computation time. Simulation using a DFN model inherently becomes more challenging as the problem scale increases, especially given the complexity of most naturally fractured reservoirs (Samardzioska and Popov 2005, Singhal and Gupta 2010).

Equivalent continuum models provide a simpler alternative in which the dual porosity geomaterial is described as a single homogenous medium, thereby reducing the input data requirements, theoretical complexity, and computational cost compared to DFN models. They are suitable provided the homogenisation process adopted can accurately capture the bulk properties of the geomaterial. In practical terms this requires a dense, highly interconnected fracture network to ensure that the flows in the fracture and matrix pore regions remain near equilibrium with each other (Berkowitz 2002). This implies that the accuracy of equivalent continuum models reduces as the partition between the fracture and matrix flows becomes more apparent.

If there is an appreciable partition between the fracture and matrix flows, it is more appropriate to employ a dual porosity model where a fracture continuum interacts with a matrix continuum. To reflect the material properties of most fractured rocks, it is generally true that the fracture continuum provides the majority of the flow capacity and the matrix continuum provides the majority of the storage capacity. In other words, the fracture continuum is more highly conductive with a lower porosity and the matrix continuum is poorly (or non-) conductive with a higher porosity (Bear 1993, Xu and Pruess 2001). Provided representative properties can be assigned to the continua and the inter-porosity flow interactions can be accurately theorised, a dual porosity model can capture the salient transport behaviour of both fractured rocks (e.g. Bai, Elsworth et al. 1993, Xu, Sonnenthal et al. 2001, Di Donato and Blunt 2004) and structured soils (e.g. Ray, Ellsworth et al. 1997, Schwartz, Juo et al. 2000).

Figure 1 shows three types of dual (or triple) porosity models that can be formulated to describe the reactive transport processes in highly fractured geomaterials (e.g. coal). A conventional dual porosity model, depicted in Figure 1a, assumes that the matrix porosity contains immobile fluids and chemicals so that there is only a single permeability, i.e. the fracture permeability. In this manner, the matrix porosity acts mainly as a sink/source to the mobile fluids and chemicals in the fractures. If the mobility

of the fluids and chemicals in the matrix porosity is considered, the result is the dual porosity, dual permeability model shown in Figure 1b. Finally, the triple porosity model illustrated in Figure 1c may be more appropriate in materials with a multi-modal matrix pore size distribution (e.g. macro-/micro-pores), as found in some coals (Clarkson and Bustin 1999, Shi and Durucan 2005).

This paper describes an advanced theoretical formulation for multiphase, multicomponent reactive chemical and gas transport in fractured geomaterials, including non-ideal gas behaviour. The dual porosity, dual permeability approach is preferred since it has been quite widely and successfully applied to this class of problems, for example in the study of coal (e.g. King, Ertekin et al. 1986, Clarkson and Bustin 1999, Shi and Durucan 2005, Ozdemir 2009, Wu, Liu et al. 2010, Thararoop, Karpyn et al. 2012), which is particularly relevant to the present work. Moreover, from the discussion given above, dual porosity models are seen to offer an attractive balance of accuracy versus practicality, requiring neither large input data sets nor excessive computational effort as the problem scale increases. Theoretical features relating to the coupled hydraulic, chemical, gas and mechanical behaviour have been included in the formulation presented. An example is the swelling of coal in response to gas adsorption, which can have a considerable feedback effect on the porosity and permeability (Clarkson and Bustin 2010).

The theoretical formulation has been implemented in an existing coupled thermal, hydraulic, chemical and mechanical (THCM) model, COMPASS, developed incrementally at the Geoenvironmental Research Centre by Thomas and co-workers (Thomas and He 1998, Cleall, Seetharam et al. 2007, Seetharam, Thomas et al. 2007, Thomas, Sedighi et al. 2012, Sedighi, Thomas et al. 2016). COMPASS has a background of high performance simulations of three-dimensional multiphase, multicomponent reactive transport in single porosity geomaterials, based on a theoretical formulation that can be described as a mechanistic approach. Geochemical reactions between components in the liquid, gas and solid phases are considered via the coupling of COMPASS to the geochemical model, PHREEQC (version 2) (Parkhurst and Appelo 1999), with the COMPASS-PHREEQC platform having been applied to study a range of problems including the performance of engineered barriers for the deep geological disposal of nuclear waste. This paper presents recent developments that extend the existing capabilities towards the aforementioned areas of geoenergy engineering, particularly carbon sequestration, achieved

principally through the introduction of the dual porosity framework and the inclusion of non-ideal gas behaviour (Hosking 2014). A series of benchmark tests have been performed on the new model to verify the correctness of the numerical implementation, with the results of these tests also being presented in this paper.

By incorporating the new developments into the pre-existing THCM framework of COMPASS, this work has yielded an advanced model of high pressure gas transport, storage and displacement for geoenery applications involving multiphase, multicomponent chemical/gas transport in dual porosity media. Beyond being a predictive tool, the mechanistic approach adopted allows for a detailed insight into the underlying coupled processes that govern the overall system behaviour, as well as providing flexibility for the continued development of the model.

Dual porosity theoretical formulation

The fracture network and porous matrix blocks are handled as distinct continua over the domain and each flow variable has fracture and matrix values at every analysis point. This yields a system of governing equations expressed in terms of six primary variables, namely, the pore water pressure in the fractures () and matrix (), the concentrations of chemical components in the aqueous phase in the fracture () and matrix (), and the concentrations of chemical components in the gas phase in the fracture () and matrix (). The gas phase is thereby modelled by considering the coupled behaviour of its constituent chemical components. Mechanical behaviour is not explicitly considered in the present work, with the feedback of deformation instead considered implicitly using constitutive relationships describing the evolution of porosity and permeability as effective stress and chemo-mechanical conditions change.

Chemical flow through the continua is considered by advection, diffusion and dispersion mechanisms. Darcy's law is used to describe the advective flow due to pressure and gravitational gradients and Fick's law is used to describe molecular diffusion, with mechanical dispersion treated analogously to molecular diffusion (Bear and Verruijt 1987). Sink/source terms are included to: i) handle equilibrium and kinetically-controlled chemical reactions, and ii) define the mass exchange processes which couple the

flows in the fracture and matrix continua.

The governing equations for coupled thermal, hydraulic and aqueous chemical behaviour in unsaturated soils have been covered in detail elsewhere (Thomas and He 1998, Cleall, Seetharam et al. 2007, Thomas, Sedighi et al. 2012, Sedighi, Thomas et al. 2016). In addition, the governing equations for the reactive transport of multicomponent gas in a single porosity unsaturated soil have been presented by Masum (2012) and Sedighi et al. (2015), assuming ideal gas behaviour. Thus, the focus of this paper is on presenting the governing equations and model development for water transfer and multicomponent reactive chemical transport in dual porosity geomaterials. In addition, the theoretical aspects implemented in the model in relation to non-ideal gas flow at high pressure are presented.

General form of the governing equations

Based on the principle of conservation of mass, the temporal derivative of the water content and chemical accumulation is equal to the spatial gradient of the relevant fluxes. Sink/source terms are included allowing for chemical reactions and mass exchange between the fracture and matrix continua. The dual porosity governing equations for water transfer (equation (1)) and the reactive transport of the dissolved or gaseous chemical component (equation (2)) are then given by:

$$\text{---} \quad (1)$$

$$\text{---} \quad (2)$$

where the subscript is the phase identifier for chemical components and becomes to denote dissolved chemical components and to denote gaseous chemical components. Similarly, the subscript is the continuum identifier and becomes to denote the fracture network and to denote the porous matrix. The superscript denotes the component number of the chemical and gas species present in the multiphase, multicomponent system. Accordingly, if or if , where and are the number of dissolved and gas components, respectively. On the left hand side of equations (1) and (2), the parameter is the volumetric water (if) or gas (if) content, is the density of liquid water, and is the sink/source term for the accumulation/generation of the

154 chemical component due to chemical reactions. The flux components are included on the right hand
 155 side of the governing equations, where \mathbf{v} represents the advective velocity, D is the effective
 156 diffusion coefficient and α is the coefficient of mechanical dispersion. In the final terms, S_1 and
 157 S_2 represent the sinks/sources for mass exchange between the continua, with S_1 if $S_1 > 0$ or S_2 if
 158 $S_2 > 0$.

159 The volumetric water or gas content, V_w , can be expressed in terms of the porosity and the degree of
 160 saturation, as:

$$(3)$$

161 where ϕ is the porosity and S_w is the degree of water or gas saturation. In the absence of water vapour,
 162 the volumetric liquid and gas contents, V_l and V_g , in a two phase system are bound by the
 163 relationship:

$$(4)$$

164 Application of Darcy's law yields the following expression for q in equations (1) and (2) (Bear and
 165 Verruijt 1987):

$$(5)$$

166 where h is the elevation and K_{rg} , the unsaturated hydraulic or gas conductivity, can be expanded to
 167 give:

$$(6)$$

168 where k is the intrinsic permeability, $k_{r,g}$ is the phase relative permeability, and μ_g is the absolute
 169 phase viscosity.

170 In determining the bulk gas phase velocity, \mathbf{v}_g , the bulk gas pressure, i.e. p_g , can be expressed in
 171 terms of the sum of the concentrations of the chemical components in the gas phase using the non-ideal
 172 gas law, given by:

(7)

173 where β is the compressibility factor, i.e. the ratio of the actual molar volume to that predicted by the
174 ideal gas law, R is the universal gas constant, and T is the temperature.

175 The effective diffusion coefficient, D_{eff} , in equation (2) is derived from the free fluid diffusion
176 coefficient, D , to account for the tortuous diffusion paths in a porous medium. This relationship can
177 be written as (Cussler 1997):

(8)

178 where τ is the tortuosity factor.

179 Mechanical dispersion in the gas phase is considered negligible compared to diffusion since gas
180 diffusion coefficients are around four orders of magnitude greater than those of dissolved chemicals
181 (Cussler 1997). Hence, $D_{eff} \approx D$. Furthermore, Therrien and Sudicky (1996) reported that mechanical
182 dispersion of dissolved chemicals in rock matrix blocks is generally weak compared to diffusion and by
183 experience may also be neglected, giving $D_{eff} \approx D$.

184 ***Porosity and permeability***

185 It is important to clearly define how the porosity and permeability of the fracture and matrix continua
186 are assigned, since characterisation tests conventionally do not (or cannot) distinguish between the
187 different pore regions (Schwartz, Juo et al. 2000). With reference to Figure 2, the matrix continuum is
188 assigned the properties of the unaltered porous rock matrix, ignoring any minor splay fractures. The
189 properties in the local region of an open fracture are more complex since fractures are not necessarily
190 clear flow conduits. Open fractures can be partially or completely blocked by infilling minerals such as
191 carbonates, quartz and clays (Ward 2002), and the presence of a fracture may also give rise to a zone of
192 altered porous matrix surrounding the discontinuity. The extent of this zone is likely to be larger in softer
193 rocks, such as coal, compared to harder rocks, such as granite. In this work, an attempt has been made
194 to assign properties to the fracture continuum that represent those of the fracture ‘zone’ comprising open
195 fractures, mineral infillings and the altered porous matrix.

The fracture continuum porosity, ϕ_f , is the fraction of the total porosity associated with the fracture zone, expressed mathematically as (Gerke and van Genuchten 1993, Zheng and Samper 2015):

$$(9)$$

where $\phi_{f,l}$ is the local fracture porosity given by the volume of the pores in the fracture zone divided by the total volume of the fracture zone, i.e. $\phi_{f,l} = V_{p,f}/V_f$. This becomes 1.0 in a clean fracture, but may be less due to mineral infillings and the presence of altered porous matrix surrounding the fracture. The parameter V_f/V_t is the volumetric weighting factor, defined as the total volume of the fracture zone divided by the total volume, i.e. V_f/V_t (Zheng and Samper 2015), analogous to the following expression if the matrix blocks have a more or less regular cubic geometry:

$$(10)$$

where a and b are the fracture aperture and matrix block half-width, respectively.

Equation (9) allows the matrix continuum porosity, ϕ_m , to be expressed in terms of the total porosity, ϕ_t , and ϕ_f , as:

$$(11)$$

Therefore, provided the values of ϕ_t , ϕ_f and V_f/V_t can be measured or estimated, the distribution of the porosity can be defined. While the measurement of ϕ_t via experimental techniques (e.g. porosimetry) does not present a major challenge, it is more difficult to distinguish between the fracture and matrix values. Nonetheless, equation (10) may be applied to estimate ϕ_f , and there are some field and laboratory techniques available to estimate the fracture porosity, i.e. ϕ_f (Singhal and Gupta 2010).

Similarly, the total intrinsic permeability, k_t , can be readily measured in the laboratory via core flooding experiments. In order to distribute the observed permeability between the dual pore regions, it is useful to consider the wide body of literature supporting the notion that the fracture network permeability is typically several orders of magnitude greater than the porous matrix permeability (Tsang and Pruess 1987, Bear 1993, Bandurraga and Bodvarsson 1999, Philip, Jennings et al. 2005). As an example, it is up to eight orders of magnitude greater in coal (Robertson 2005). It is therefore assumed that the total

permeability, k_f , determined in a laboratory test belongs to the fracture network, i.e. k_f , where k_m is the intrinsic permeability of the fracture network. The permeability of the fracture continuum, k_{fc} , is then conveniently expressed as:

$$(12)$$

The local matrix permeability, k_m , is subsequently set to several orders of magnitude less than k_f and may be determined via model calibration against laboratory data (Bandurraga and Bodvarsson 1999). The permeability of the matrix continuum, k_{mc} , is given by:

$$(13)$$

Equations (9) to (13) together define the approach used to assign the porosity and permeability under the dual continuum framework considered in this work.

Mass exchange between the fracture and matrix continua

Expressions for the sink/source terms controlling the exchange rates of inter-porosity water and chemical components in the liquid and gas phases are presented in this section. It is assumed that quasi-steady state distributions of pore water pressure and chemical concentrations prevail across the porous matrix block thickness at all times. This assumption is strictly only valid once the pressure or concentration front due to a change in conditions in the fracture network has reached the centre of the matrix block, and so may not be valid over all time scales (Lemonnier and Bourbiaux 2010). However, it allows the mass exchange terms to be conveniently expressed as linear functions of the differences between the fracture and average matrix pressures and concentrations (Barenblatt, Zheltov et al. 1960, Warren and Root 1963, Hassanzadeh, Pooladi-Darvish et al. 2009).

The mass exchange of water is treated as an advective flow, whereas for chemicals both advective and diffusive mechanisms are considered (Gwo, Jardine et al. 1995, Ray, Ellsworth et al. 1997, Kohne, Mohanty et al. 2004). Accordingly, first-order mass exchange terms can be written for water and the dissolved chemical or gas component, expressed in a general form as (Gwo, Jardine et al. 1995, Ray, Ellsworth et al. 1997):

$$— \quad (14)$$

$$— \quad (15)$$

241 where C_m is the resident concentration, for which $C_m = C_f$ if mass exchange is from the fracture
 242 continuum to the matrix continuum and $C_m = C_f$ if the exchange is reversed. λ_a and λ_d are the first-
 243 order exchange rates relating to advection and diffusion, respectively. These parameters can be expanded
 244 considering the relevant geometrical and material properties, including the matrix block shape and
 245 dimensions, the permeability and diffusivity of the fracture-matrix interface (i.e. the fracture zone in
 246 Figure 2) and the fluid transport properties, giving expressions of the form (Schwartz, Juo et al. 2000):

$$— \quad (16)$$

$$— \quad (17)$$

247 where b is the typical half-width of a matrix block, K_{fm} is the effective hydraulic conductivity between
 248 the fracture and matrix pore regions, and α is a dimensionless factor related to the geometry of the
 249 matrix blocks, which can range from 3 for rectangular slabs to 15 for spherical aggregates (Gerke and
 250 van Genuchten 1993, Kohne, Mohanty et al. 2004), but otherwise in practice may also be lumped with
 251 the remaining parameters in equations (16) and (17) to form an empirical coefficient for calibration
 252 using observed laboratory or field data. Gerke and van Genuchten (1993) evaluated a number of methods
 253 for obtaining α and concluded that an arithmetic mean approach is the most practical, giving:

$$— \quad (18)$$

254 ***Chemical reactions***

255 Previous works have coupled the transport model (COMPASS) with chemical models, for example
 256 MINTEQA2 (Cleall, Seetharam et al. 2007, Seetharam, Thomas et al. 2007) and PHREEQC (version 2)
 257 (Thomas, Sedighi et al. 2012, Sedighi, Thomas et al. 2015), enabling the study of a range of
 258 geoenvironmental and geoenergy problems involving multiphase, multicomponent chemical transport
 259 in single porosity geomaterials with homogenous and heterogeneous reactions. While an extension of

this coupling to the dual porosity framework is not part of the present developments, which are more concerned with transport processes than chemical reactions, it is considered for future development as has already been accomplished in other applications of COMPASS (e.g. Sedighi, Thomas et al. 2016). Nonetheless, the adsorption and desorption of multicomponent chemicals is important in geoenery applications including carbon sequestration in coal, enhanced hydrocarbon recovery, and unconventional gas exploration. Hence, the development of the chemical reactions presented is limited here to adsorption and desorption in the solid, and it is acknowledged that a more general geochemical modelling approach will be required when a further complicated multiphase, multicomponent system is of interest.

The sink/source terms, S_i , in equations (1) and (2) can be expanded to give:

$$S_i = -\rho_b \frac{dQ_i}{dt} \quad (19)$$

$$S_i = -\rho_b \frac{dQ_i}{dt} \quad (20)$$

where ρ_b is the dry bulk density, Q_i is the adsorbed amount of the i chemical component. The factors f_m and f_f are used to partition the adsorption sites between the fracture network and porous matrix blocks.

Adsorption inherently depends on the available surface area of the adsorbent (solid phase) over which interactions with the adsorbate can occur. In fractured rock, such as coal, the majority of the surface area exists in the porous matrix blocks (Clarkson and Bustin 2010). It is therefore assumed that the matrix continuum provides all of the adsorption capacity, so that equations (19) and (20) become:

$$S_i = -\rho_b \frac{dQ_i}{dt} \quad (21)$$

$$S_i = -\rho_b \frac{dQ_i}{dt} \quad (22)$$

A kinetic chemical reaction is formulated to describe the adsorption/desorption phenomena, similar to that presented in the previous section for inter-porosity mass exchange. This yields a first-order model describing sorption in the matrix continuum, as (King, Ertekin et al. 1986):

(23)

where $\frac{dq}{dt}$ is the rate of adsorption/desorption and q_{eq} is the adsorbed amount at equilibrium with the free-phase adsorbate. q_{eq} is evaluated using an appropriate adsorption isotherm, which may be a simple linear relationship or a nonlinear relationship such as a Langmuir isotherm.

Multiphase coupling

Changes in the degree of water saturation, S_w , influence the physical and chemical behaviour in partially saturated fractured rock, most notably through feedback to the phase relative permeability, $k_{r,w}$. An important characteristic of fractured rock is that the fracture network is more free-draining than the porous rock matrix, making it important to define the water retention behaviour appropriately in the respective continua. The rate of change of S_w is affected by the difference between pore water pressure and pore gas pressure, known as matric suction (Mitchell and Soga 2005), as well as changes to the void ratio caused by deformation (Gallipoli, Wheeler et al. 2003). The effect of the latter is less clearly defined and often neglected in the study of fairly rigid porous media (Mašin 2010), such as coal, giving:

(24)

where u is the matric suction, expressed in terms of the primary variables with substitution from equation (7), leading to (Mitchell and Soga 2005):

(25)

From equations (24) and (25), the temporal derivative of the degree of water saturation can be expanded to yield:

(26)

where the partial derivative of S_w with respect to u is analogous to the specific water capacity and defined as the gradient of the water retention curve via the van Genuchten (1980) model, given by:

(27)

where θ_e is the effective volumetric water content, and θ_r and θ_s are the residual and saturated volumetric water contents, respectively, and α , n and k_r () are constants based on the water retention characteristics of each continuum.

The phase relative permeability, $k_{r,p}$, is evaluated from k_r , giving:

(28)

where the function on the right hand side is given by the van Genuchten-Mualem model (Mualem 1976, van Genuchten 1980) for k_r , with the extended model by Parker et al. (1987) used for $k_{r,p}$, giving:

(29)

(30)

The main limitation of this approach in the dual porosity framework is the lack of experimental data available to determine the parameters of the hydraulic functions given in equations (27), (29) and (30). Nonetheless, it is possible to estimate water retention curves for the fracture and matrix continua based on the characteristics of the respective pore regions, most notably the pore size distributions (e.g. Zhang and Fredlund 2003). Moreover, Köhne et al. (2002) presented a procedure for estimating the dual permeability water retention and conductivity functions using bulk soil data, based on the notion of volumetric weighting. Since volumetric weighting is also used in this formulation, future work could look at applying the Köhne et al. procedure for modelling fractured rock.

Further to the water retention behaviour and phase relative permeability described in this section, the option to include gas-liquid phase transformations exists through the coupling of COMPASS with PHREEQC. However, this option has not been explored in the present work owing to the focus on carbon sequestration in coalbeds, in which the adsorbed phase tends to dominate gas storage. Coalbeds are also quite often dewatered during primary methane recovery prior to the injection of carbon dioxide (CO₂) for enhanced recovery. Further applications of the model considering problems such as carbon sequestration in saline aquifers would require an elaboration of the gas-liquid phase transformation.

Gas properties

Appropriate constitutive relationships are employed in the model to accurately describe the evolution of the key gas transport properties as the pressure, temperature and composition vary. In relation to the formulation described above, these properties are the non-ideal gas compressibility and the gas viscosity. Non-ideal gas compressibility is considered using the Peng and Robinson (1976) equation of state (EoS) with van der Waals mixing rules. This approach has been widely applied with a proven accuracy and requires little input data (Wei and Sadus 2000). The EoS expresses the bulk gas pressure as:

$$\frac{P}{RT} = \frac{1}{V - b} - \frac{a}{V(V + b)} \quad (31)$$

where b is the effective volume of the molecules contained in one mole of bulk gas and a is a coefficient accounting for the intermolecular interactions in the mixture, both of which are obtained via the van der Waals mixing rules (Kwak and Mansoori 1986). The parameter V is the molar volume of the gas mixture predicted by the ideal gas law.

For an ideal gas, the factors a and b are zero and equation (31) reduces to the ideal gas law. However, the ideal gas law does not accurately describe the pressure-volume-temperature characteristics of gas under the majority of conditions (Dake 1978). Deviations from the ideal gas law are described by the compressibility factor, Z , which is determined by rewriting equation (31) as a cubic equation according to Peng and Robinson (1976):

$$Z^3 - Z^2 + \frac{a}{RT}Z - \frac{ab}{RT} = 0 \quad (32)$$

where:

$$a = \sum_i \sum_j y_i y_j a_{ij} \quad (33)$$

$$b = \sum_i y_i b_i \quad (34)$$

Of the three roots to Equation (32), the selection of Z depends on the number of real roots and the phase composition of the pore fluid, as outlined by Chen et al. (2006).

Gas mixture viscosity is included using the semi-empirical model proposed by Chung et al. (1988). The

model is based on the kinetic theory of gases in combination with empirical density-dependent functions and has been chosen ahead of simpler interpolative models because it describes the evolution of the mixture viscosity not only with composition, but also with pressure and temperature. Moreover, the model retains accuracy near the critical point and has shown absolute deviations of no more than 9% for non-polar dense gas mixtures. The model is expressed as:

(35)

where μ_0 is a function of the gas mixture viscosity at low pressure and μ_{∞} is an adjustment for dense gases. These terms are fully expanded and described in Chung et al. (1988).

Deformation feedback

While mechanical behaviour is not explicitly considered in this work, the feedback of deformation on fluid transport is considered implicitly since it can be important in some cases of dual porosity flow. For example, the porosity and permeability of rock can be strongly influenced by effective stress changes and certain chemo-mechanical phenomena, including sorption-induced swelling/shrinking of the rock matrix. These changes in porosity and permeability are described in a general form as (Xu and Pruess 2001):

(36)

where the subscript i denotes the initial condition, σ_e is the effective stress, and ϵ_t is the total sorption strain of the matrix blocks, equal to the sum of the strains induced by each component, i.e. $\epsilon_t = \sum \epsilon_i$.

Relationships in the form of equation (36) apply in the study of geomaterials which can be described as fractured sorptive elastic media (e.g. coal). A number of relationships have been presented in the literature (Palmer and Mansoori 1988, Shi and Durucan 2004, Robertson and Christiansen 2008), with an adsorption isotherm-type relationship conventionally being used to obtain ϵ_i . This approach has proven accurate based on comparison with the results of experimental studies (Harpalani and Chen 1995, Levine 1996).

Computational approach

Substitution of the pore fluid velocity from equation (5), the porosity and permeability relationships from equations (9) to (13), the mass exchange sink/source terms from equations (14) and (15), and the chemical reaction sink/source term from equations (22) and (23) into equations (1) and (2) produces equations of the form:

$$\frac{\partial}{\partial t} \left(\frac{\rho_w}{\rho_w} \right) + \frac{\partial}{\partial x} \left(\frac{\rho_w}{\rho_w} \right) = \frac{\partial}{\partial x} \left(\frac{\rho_w}{\rho_w} \right) \quad (37)$$

$$\frac{\partial}{\partial t} \left(\frac{\rho_w}{\rho_w} \right) + \frac{\partial}{\partial x} \left(\frac{\rho_w}{\rho_w} \right) = \frac{\partial}{\partial x} \left(\frac{\rho_w}{\rho_w} \right) \quad (38)$$

where α and β are lumped coefficients of the governing equations, and γ and δ are terms representing the gravitational body forces for the water and chemical terms, respectively.

The numerical solution of the governing equations is achieved by applying the finite element method with Galerkin weighted residuals for spatial discretisation and an implicit mid-interval backward-difference scheme for temporal discretisation. This solution procedure follows works on the coupled THM and THCM behaviour of single porosity media presented in detail by Thomas and He (1998) and Seetharam et al. (2007). A time splitting technique, namely the sequential non-iterative approach (SNIA), is employed in which the conservative transport formulation, mass exchange and chemical reactions are solved sequentially in each time step. In other words, each time step first involves solving the conservative transport equations in each continuum assuming no mass exchange and no reactions. Once this system has converged, the values of the primary flow variables are updated in the mass exchange and chemical reaction modules. Although such an approach has proven successful for sufficiently small time steps (Seetharam, Thomas et al. 2007, Thomas, Sedighi et al. 2012), the use of a split time step via the SNIA is acknowledged as a limitation of the present work and other approaches, including the sequential iterative approach (SIA) and global implicit approach, are available.

Model verification

A set of verification tests has been performed to assess the correctness of the numerical implementation

of the theoretical and numerical developments in the model, with benchmarks provided by analytical or alternative numerical solutions presented in the literature. The first test deals with multiphase flow, considering the evolution of the degree of saturation as water and gas flow in a partially saturated porous medium. In the second test, two simulations are performed for multicomponent gas transport at high pressure with kinetically-controlled adsorption/desorption. The results are compared with the results of an alternative numerical model presented in the literature. This also provides an opportunity to verify the performance of the constitutive relationships implemented for non-ideal gas behaviour, most notably in the case of CO₂ transport, which is highly non-ideal under the simulation conditions. A further sets of tests is then presented to examine the coupling scheme (SNIA) between the chemical transport and inter-porosity mass exchange modules of the developed model.

Multiphase flow

This section presents a verification test (Test I) for the coupled flow of water and ideal gas in a single porosity medium. The test considers a two-dimensional domain of 1 m length and 0.1 m height, spatially discretised using 200 quadrilateral elements concentrated towards the upstream and downstream faces. Under the simulation conditions shown in Figure 3, the isothermal system is initially partially saturated with fixed pore water and gas pressures at the downstream boundary. An influx of gas begins at the upstream boundary after 1 day, rising linearly from zero to 0.01 mol s⁻¹ by the end of the simulation period. The aim of the test is to verify the initial ingress of water from the downstream boundary and its subsequent displacement due to the gas influx at the upstream boundary.

A benchmark for the simulation results is provided by comparing the predicted changes in the degree of water saturation to the conditions expected with reference to the water retention and relative permeability functions in Figure 4 and Figure 5, respectively, based on the material parameters provided in Table 1. Similar to the approach of Köhne et al. (2002), the parameters adopted for the hydraulic functions are taken from van Genuchten (1980) and compare an un-fractured rock matrix to a fine-textured porous medium, in this case “Touchet silt loam”.

Figure 6 shows the predicted evolution of the degree of water saturation, S_w , at the mid-point of the domain, i.e. 0.5 m. The first point of reference for S_w is under the initial conditions, given as 0.81

by the flat section of Figure 6 at early times before water ingress from the downstream boundary. Considering the initial suction of 18.1 kPa, the initial θ predicted in the numerical simulation agrees with the expected value given by Figure 4. After this initial period, θ rises towards the fully saturated condition as the flow of water from the downstream boundary reaches the mid-point of the domain, with this condition prevailing until the onset of gas injection after 1 day (86400 s). As expected, the gas influx from the upstream boundary causes a decline in θ , initially sharp before tailing as it tends towards the residual value of 0.405. Noting the logarithmic scales used for the time axes, the tailing of θ in Figure 6 as the gas flux increases is comparable to that of the water retention curve in Figure 4. In other words, θ is declining in the manner expected as the pore gas pressure in the system steadily increases.

Test I demonstrates the capability for simulating two-phase flow under the conditions considered, namely, the re-saturation of a partially saturated porous medium and the subsequent displacement of pore water through gas injection. The test therefore forms the basis for further verification of multiphase flow in future work, particularly for the dual porosity case, where inter-porosity flow and the bi-modal nature of the hydraulic functions are of relevance.

Multicomponent reactive gas transport at high pressure

Two scenarios of high pressure gas injection and displacement are simulated and the results are compared with those obtained in the numerical modelling study by Pini et al. (2011). Both scenarios deal with the enhanced displacement of methane (CH_4) due to gas injection in a 100 m long coalbed with unit cross section. The first scenario (Test II-a) considers the displacement of CH_4 during CO_2 injection, i.e. carbon sequestration, whereas the second scenario (Test II-b) considers nitrogen (N_2) injection.

Since the exercise is mainly concerned with verifying the non-ideal, multicomponent reactive gas transport behaviour, the system is treated as a single porosity medium with kinetically-controlled adsorption/desorption. The domain is discretised using 500 equally-sized 4-noded quadrilateral elements and is initially saturated with CH_4 at a pressure of 1.5 MPa at a temperature of 318 K. The amount of gas stored in the adsorbed phase is initially at equilibrium with the free gas phase and calculated using

the extended Langmuir isotherm (ELI), which for the component in a gas mixture is given by (Ruthven 1984):

$$(39)$$

where is the Langmuir capacity and is the reciprocal of the Langmuir pressure. Equation (39) is used in equation (23) to calculate the changes in the adsorbed phase as CO₂ or N₂ displaces CH₄ in the coalbed.

The injection boundary pressure for CO₂ and N₂ is 4 MPa at , with an atmospheric pressure production boundary condition prescribed at . A schematic representation of this system is

Injection boundary conditions	Initial conditions	Production boundary conditions
Test II-a: $c_g^{CO_2} = 1,881.9 \text{ mol m}^{-3}$ Test II-b: $c_g^{N_2} = 1,522.5 \text{ mol m}^{-3}$	Free gas (mol m ⁻³): $c_g^{CO_2} = c_g^{N_2} = 0.0$ $c_g^{CH_4} = 582.4$ Adsorbed gas (mol kg ⁻¹): $s_{gM}^{CO_2} = s_{gM}^{N_2} = 0.0$ $s_{gM}^{CH_4} = 0.75$	$RT \sum_{j=1}^{n_g} c_g^j = 0.1 \times 10^6 \text{ Pa}$ $\sum_{j=1}^{n_g} \frac{\partial c_g^j}{\partial t} = 0.0$

provided in

Figure 7, where the stated pressures are expressed as the equivalent gas concentrations. All of the properties required in the Peng and Robinson EoS have been taken from IEAGHG (2011).

As adopted by Pini et al. (2011), in equation (36) is expanded using the relationship proposed by Gilman and Beckie (2000), giving:

$$(40)$$

where is Poisson's ratio, is Young's modulus, is the confining pressure, and the coefficients and are defined in Table 2.

along with a summary of the other physical and chemical parameters used in the simulations, including the component viscosities, , adopted from Linstrom and Mallard (2001). The parameter is the swelling fraction, i.e. , with given by:

where ϵ_L is the Langmuir strain and $\frac{1}{P_L}$ is the reciprocal of the Langmuir swelling pressure.

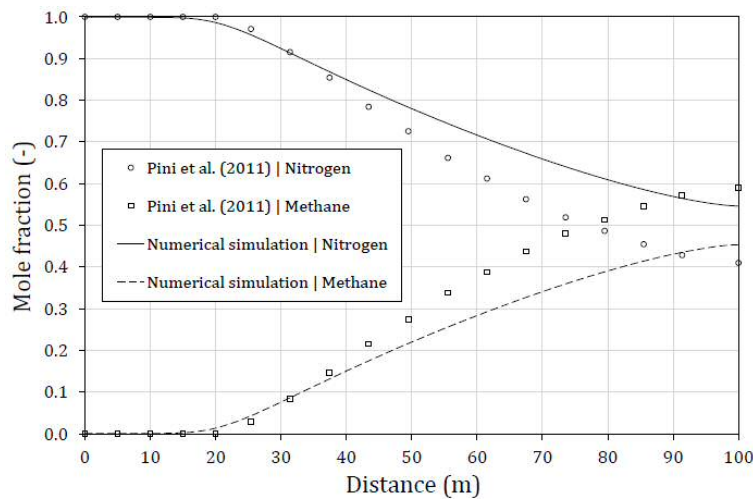
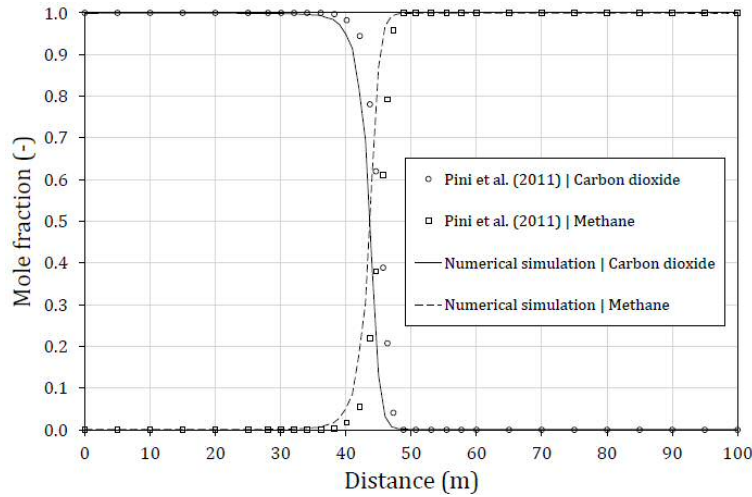


Figure 8 and

Figure 9 show the results obtained using the numerical model after 42 days of analysis for Tests II-a and II-b, respectively. There are considerable differences in the predicted CH_4 displacement profiles, with CO_2 producing a sharper yet less advanced front compared to the results for N_2 injection. Whilst both gases physically sweep free CH_4 from the pore space, these differences arise due to the sorption and sorption-induced swelling phenomena. In particular: i) coal has a higher affinity for CO_2 adsorption than for CH_4 , whereas a lower affinity for N_2 adsorption, and ii) CO_2 adsorption results in a swelling-induced permeability loss. Hence, in Test II-b, N_2 does not displace the adsorbed CH_4 as efficiently as CO_2 in

Test II-a, less N_2 is immobilised via adsorption, and the system permeability remains higher. The displacement of the free CH_4 therefore occurs more rapidly in Test II-b, causing breakthrough of N_2 at the production boundary. The significant spreading of the injection front can be attributed to the more gradual displacement of the adsorbed CH_4 by N_2 compared to CO_2 .

In both tests, the results show agreement with the benchmarks provided by Pini et al. (2011). A degree of deviation is noted and may be attributed to differences in the prescribed gas viscosities. Whereas Pini et al. adopted Wilke's dilute gas mixture method (Poling, Prausnitz et al. 2001) using unspecified pure component viscosities, the same method has been used here for Test II but with viscosities taken from Linstrom and Mallard (2001). Hence, there may be some degree of disagreement between these viscosities and those used by Pini et al. Based on the results achieved and under the conditions of the problems described, it can be reasonably concluded that the transport behaviour of multicomponent gas, including kinetically-controlled adsorption/desorption, is accurately implemented in the numerical model.

Dual porosity, dual permeability chemical transport and exchange

This section presents three verification tests (Tests III-a, III-b and III-c) for dual porosity, dual permeability chemical transport. The tests consider the transport of a chemical component in a fully saturated dual porosity geomaterial subject to steady state water flow, equilibrium adsorption, and various mass exchange rates. The simulation results are presented as chemical breakthrough curves at an analysis point and comparisons are made with the results obtained by Šimunek and van Genuchten (2008) using the HYDRUS-1D numerical model.

A two-dimensional domain of 1 m length and 0.1 m height is spatially discretised using 50 equally-sized 4-noded quadrilateral elements, with the analysis point for chemical breakthrough located at m. Each test is performed for a simulation period of 10 days with initial and maximum time steps of 100 and 3,600 seconds, respectively. The arbitrary chemical component is introduced into the system with a fixed concentration of mol m^{-3} at m and a far field concentration of mol m^{-3} at m.

Diffusion of the chemical was not considered by Šimunek and van Genuchten (2008) and equilibrium

adsorption was modelled using a retardation factor, R . Under these conditions, the governing equation in equation (2) reduces to:

$$\frac{\partial C}{\partial t} + \frac{\partial C}{\partial x} = \frac{D}{L} \frac{\partial^2 C}{\partial x^2} \quad (42)$$

with the coefficient of mechanical dispersion, D , given by:

$$D = \alpha_L v + D_m \quad (43)$$

where α_L is the longitudinal dispersivity.

Since the pore water pressures in the fracture and matrix continua are assumed to remain equilibrated, the advective component of chemical mass exchange in equation (15) becomes zero. Šimunek and van Genuchten (2008) then used a lumped mass exchange rate for the diffusive component, given by:

$$M = \lambda C \quad (44)$$

with the mass exchange rate, λ , defined as:

$$\lambda = \frac{M}{C} \quad (45)$$

$$\lambda = \frac{M}{C} \quad (46)$$

where M is the chemical mass exchange rate.

HYDRUS-1D handles the dual porosity, dual permeability framework in a slightly different form to that described in this work. Based on the work of Gerke and van Genuchten (1993), the material parameters in the governing equations are defined at the local scale (e.g. α_L), whereas in this work they are defined at the bulk scale (e.g. α_L). A discussion on the background and procedures for converting between the local and bulk scales was provided in the “Porosity and permeability” section of the theoretical formulation. Importantly, both approaches produce the same overall behaviour.

As an example, Šimunek and van Genuchten (2008) set α_L as 0.1 and prescribed steady pore water velocities of 1 m s^{-1} and 1 m s^{-1} at the local scale in the fracture and matrix continua, respectively. The corresponding bulk scale hydraulic conductivities are back-calculated from

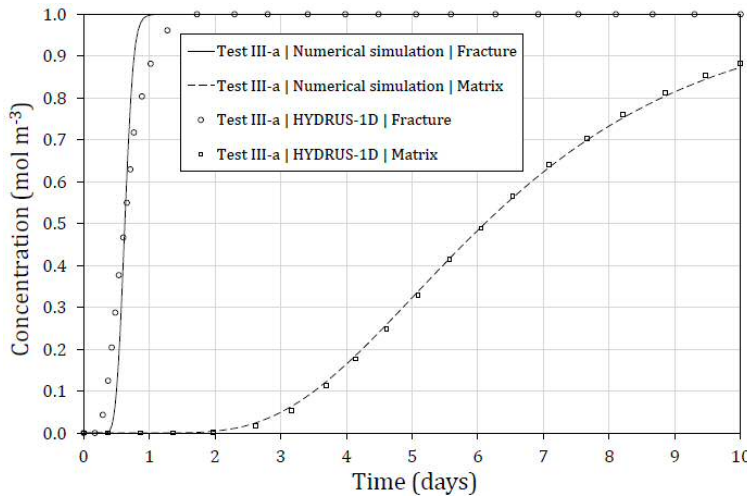
509 these velocities using equation (5) (m) by prescribing a pressure drop of 10 Pa over the length
510 of the domain and using to convert to the equivalent bulk scale conductivities, giving:

$$\text{---} \quad (47)$$

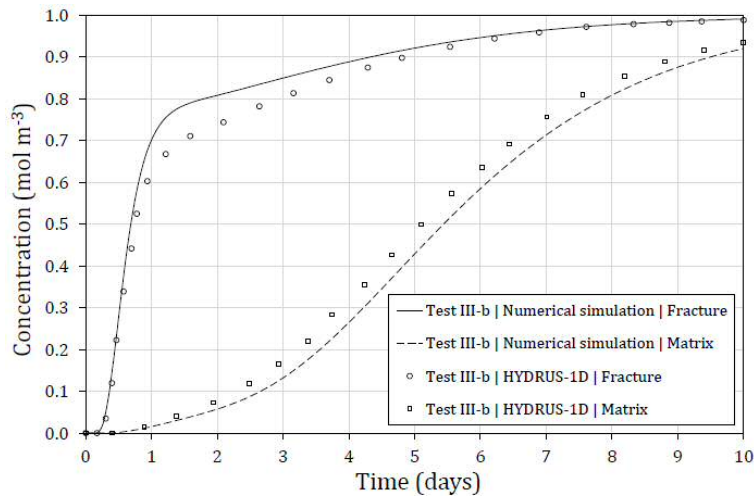
$$\text{---} \quad (48)$$

511 where is the pore water velocity at the local pore region scale, is the length of the domain, i.e. 1 m,
512 and Pa, giving m s⁻¹ and m s⁻¹.

513 Table 3 provides a summary of the physical and chemical parameters used in the simulations for
514 verification Tests III-a, III-b and III-c. No mass exchange is considered in Test III-a so that the fracture
515 and matrix continua behave as independent flow conduits. The effects of different mass exchange rates
516 are then examined in Tests III-b and III-c, with the rate in Test III-c being five times greater than that
517 applied in Test III-b.



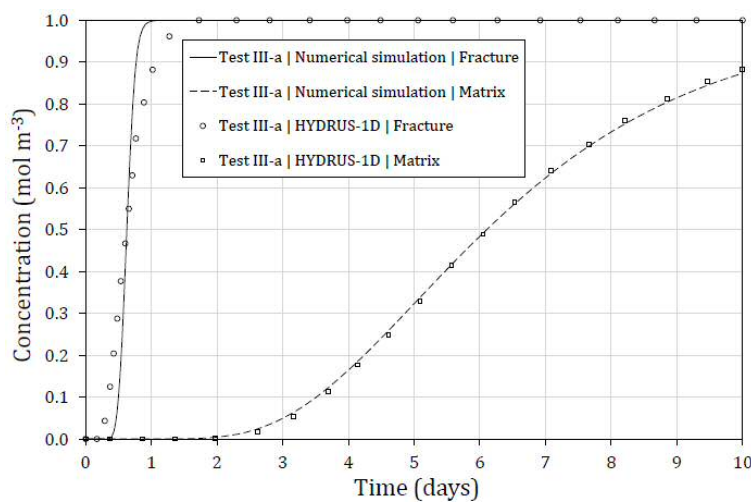
519 Figure 10 shows the chemical breakthrough in the fracture and matrix continua with no mass exchange.
520 It can be seen that the breakthrough in the fracture continuum occurs earlier and is sharper than in the
521 matrix continuum. This results from a combination of the higher pore water velocity in the fracture
522 continuum and the considerably lower chemical storage capacity provided by its porosity.



523 The breakthrough curves in

524 Figure 11 and Figure 12 show the role of lower (Test III-b) and higher (Test III-c) mass exchange rates
 525 on chemical transport, respectively. Most notable are the more gradual fracture breakthrough and earlier
 526 matrix breakthrough which follow an increase in the mass exchange rate. This is the expected trend
 527 since the rapid chemical advance in the fracture continuum resulted in higher fracture concentrations
 528 than matrix concentrations, thereby driving chemical exchange from the fracture continuum into the
 529 matrix continuum. At higher mass exchange rates the resistance to these flow interactions between the
 530 continua reduces. The breakthrough curves then tend towards that which would be predicted by an
 531 equivalent single porosity, single permeability model.

532 Having analysed the breakthrough curves in



533

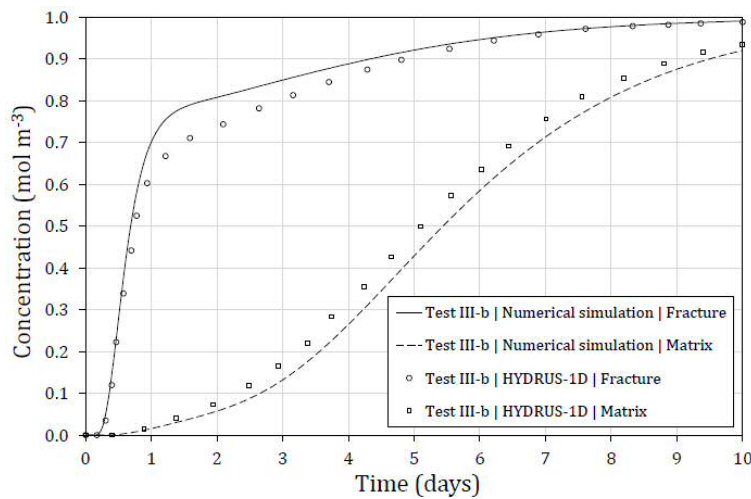


Figure 10,

Figure 11 and Figure 12, it can be concluded that the sink/source term for mass exchange between the fracture and matrix continua produces the expected behaviour. Further confidence is provided by the close agreement of the results with the benchmarks provided by Šimunek and van Genuchten (2008) for HYDRUS-1D.

The set of verification tests presented above establish a good level of confidence regarding the accurate numerical implementation of the theoretical framework for reactive flow in dual porosity geomaterials. Building upon this work, the application of the model in the study of geoenery applications, such as geological carbon sequestration, will be considered in future work.

Conclusions

A theoretical and numerical modelling platform has been developed for studying the coupled behaviour of geoenery systems involving the transport, storage, and displacement of multiphase, multicomponent chemicals and gas in the deep geoenvironment. Specifically, the capabilities of a coupled thermal, hydraulic, chemical and mechanical (THCM) model have been enhanced to consider hydraulic, chemical, gas and deformation behaviour based on a dual porosity, dual permeability framework.

Appropriate constitutive relationships have been included to provide an accurate description of the properties of high pressure, non-ideal gas mixtures. Additional theoretical features have also been included to allow the study of physically and chemically complex geomaterials, such as coal. There are terms in the governing equations to describe equilibrium or kinetically-controlled adsorption/desorption

in the porous matrix, and an implicit approach has been employed to consider the feedback of physico- and chemo-mechanical deformation on the transport processes.

A set of verification tests of the model provided further confidence in: i) the approach taken to multiphase coupling, ii) the accuracy of the numerical implementation of the dual porosity governing equations, and iii) the effectiveness of the technique employed for coupling the transport module with the mass exchange and chemical reaction modules. The tests have been accompanied by analyses of the relevant behaviour considered, lending further confidence to the verification process.

The compositional structure of the model developed provides a flexible scientific tool for both present and future applications in the geoenergy field. The developments are most relevant to the simulation of high pressure gas transport, storage, and displacement in fractured rock during geological carbon sequestration, the enhanced recovery of conventional oil and gas, the exploration of unconventional gas, and the deep geological disposal of nuclear waste. Nonetheless, the model can be more generally applied in the study of other geoenvironmental problems in structured soils, including groundwater flow and contaminant transport. Hence, future work will focus on the application of the model to enhance the current understanding in these geoenergy and geoenvironmental areas.

Acknowledgements

The financial support provided by the Welsh European Funding Office (WEFO) for the PhD studentship of the first author, through the Seren project, is gratefully acknowledged.

References

- Bai, M., Elsworth, D. and Roegiers, J. C. 1993. Multiporosity Multipermeability Approach to the Simulation of Naturally Fractured Reservoirs. *Water Resources Research*, **29**(6): 1621-1633.
- Bandurraga, T. M. and Bodvarsson, G. S. 1999. Calibrating hydrogeologic parameters for the 3-D site-scale unsaturated zone model of Yucca Mountain, Nevada. *Journal of Contaminant Hydrology*, **38**(1-3): 25-46.
- Barenblatt, G. I., Zheltov, I. P. and Kochina, I. N. 1960. Basic concepts in the theory of seepage of homogenous liquids in fissured rocks (strata). *Journal of Applied Mathematics and Mechanics*, **24**(5): 1286-1303.
- Bear, J., Ed. 1993. Modeling flow and contaminant transport in fractured rocks. Flow and contaminant transport in fractured rock, Academic Press, Inc.
- Bear, J. and Verruijt, A. 1987. Modeling groundwater flow and pollution. Dordrecht, The Netherlands, D. Reidel Publishing Company.
- Berkowitz, B. 2002. Characterizing flow and transport in fractured geological media: A review. *Advances in Water Resources*, **25**(8-12): 861-884.
- Chen, Z., Huan, G. and Ma, Y. 2006. Computational Methods for Multiphase Flows in Porous Media. Philadelphia, Society for Industrial and Applied Mathematics.
- Chung, T. H., Ajlan, M., Lee, L. L. and Starling, K. E. 1988. Generalized Multiparameter Correlation for Nonpolar and Polar Fluid Transport-Properties. *Industrial & Engineering Chemistry Research*, **27**(4): 671-679.
- Clarkson, C. R. and Bustin, R. M. 1999. The effect of pore structure and gas pressure upon the transport properties of coal: a laboratory and modeling study. 2. Adsorption rate modeling. *Fuel*, **78**(11): 1345-1362.
- Clarkson, C. R. and Bustin, R. M. 2010. Coalbed methane: current evaluation methods, future technical challenges. SPE Unconventional Gas Conference. Pittsburgh, Pennsylvania.
- Cleall, P. J., Seetharam, S. C. and Thomas, H. R. 2007. Inclusion of some aspects of chemical behavior of unsaturated soil in thermo/hydro/chemical/mechanical models. I: Model development. *Journal of Engineering Mechanics-Asce*, **133**(3): 338-347.
- Cussler, E. L. 1997. Diffusion: mass transfer in fluid systems. Cambridge, Cambridge University Press.

- Dake, L. P. 1978. Fundamentals of reservoir engineering. Amsterdam, The Netherlands, Elsevier.
- Di Donato, G. and Blunt, M. J. 2004. Streamline-based dual-porosity simulation of reactive transport and flow in fractured reservoirs. *Water Resources Research*, **40**(4).
- Gallipoli, D., Wheeler, S. and Karstunen, M. 2003. Modelling the variation of degree of saturation in a deformable unsaturated soil. *Géotechnique*, **53**(1): 105-112.
- Gerke, H. H. and van Genuchten, M. T. 1993. A Dual-Porosity Model for Simulating the Preferential Movement of Water and Solutes in Structured Porous-Media. *Water Resources Research*, **29**(2): 305-319.
- Gerke, H. H. and van Genuchten, M. T. 1993. Evaluation of a First-Order Water Transfer Term for Variably Saturated Dual-Porosity Flow Models. *Water Resources Research*, **29**(4): 1225-1238.
- Gilman, A. and Beckie, R. 2000. Flow of coal-bed methane to a gallery. *Transport in Porous Media*, **41**(1): 1-16.
- Gwo, J. P., Jardine, P. M., Wilson, G. V. and Yeh, G. T. 1995. A Multiple-Pore-Region Concept to Modeling Mass-Transfer in Subsurface Media. *Journal of Hydrology*, **164**(1-4): 217-237.
- Harpalani, S. and Chen, G. L. 1995. Estimation of Changes in Fracture Porosity of Coal with Gas Emission. *Fuel*, **74**(10): 1491-1498.
- Hassanzadeh, H., Pooladi-Darvish, M. and Atabay, S. 2009. Shape factor in the drawdown solution for well testing of dual-porosity systems. *Advances in Water Resources*, **32**(11): 1652-1663.
- Hosking, L. J. 2014. Reactive transport modelling of high pressure gas flow in coal, Cardiff University.
- IEAGHG 2011. Effects of impurities on geological storage of CO₂, International Energy Agency Environmental Projects Ltd.
- King, G. R., Ertekin, T. and Schwerer, F. C. 1986. Numerical simulation of the transient behaviour of coal-seam degasification wells. *Society of Petroleum Engineers Formation Evaluation*, **1**(2): 165-183.
- Köhne, J. M., Köhne, S. and Gerke, H. 2002. Estimating the hydraulic functions of dual-permeability models from bulk soil data. *Water resources research*, **38**(7).
- Kohne, J. M., Mohanty, B. P., Simunek, J. and Gerke, H. H. 2004. Numerical evaluation of a second-order water transfer term for variably saturated dual-permeability models. *Water Resources Research*, **40**(7).

- Kwak, T. Y. and Mansoori, G. A. 1986. Vanderwaals Mixing Rules for Cubic Equations of State - Applications for Supercritical Fluid Extraction Modeling. *Chemical Engineering Science*, **41**(5): 1303-1309.
- Lemonnier, P. and Bourbiaux, B. 2010. Simulation of Naturally Fractured Reservoirs. State of the Art-Part 2–Matrix-Fracture Transfers and Typical Features of Numerical Studies. *Oil & Gas Science and Technology–Revue de l'Institut Français du Pétrole*, **65**(2): 263-286.
- Levine, J. R. 1996. Model study of the influence of matrix shrinkage on absolute permeability of coal bed reservoirs. In Gayer, R. & Harris, I. (eds.) *Coalbed methane and coal geology*: 197-212.
- Linstrom, P. J. and Mallard, W. G. 2001. NIST Chemistry WebBook; NIST Standard Reference Database No. 69. from <http://webbook.nist.gov/>.
- MacQuarrie, K. T. B. and Mayer, K. U. 2005. Reactive transport modeling in fractured rock: A state-of-the-science review. *Earth-Science Reviews*, **72**(3-4): 189-227.
- Mašín, D. 2010. Predicting the dependency of a degree of saturation on void ratio and suction using effective stress principle for unsaturated soils. *International Journal for Numerical and Analytical Methods in Geomechanics*, **34**(1): 73-90.
- Masum, S. A. 2012. Modelling of reactive gas transport in unsaturated soil – a coupled thermo-hydro-chemical-mechanical approach PhD Thesis, Cardiff University.
- Mitchell, J. K. and Soga, K. 2005. *Fundamentals of soil behavior*.
- Mualem, Y. 1976. A new model for predicting the hydraulic conductivity of unsaturated porous media. *Water resources research*, **12**(3): 513-522.
- Ozdemir, E. 2009. Modeling of coal bed methane (CBM) production and CO₂ sequestration in coal seams. *International Journal of Coal Geology*, **77**(1-2): 145-152.
- Palmer, I. and Mansoori, J. 1988. How permeability depends on stress and pore pressure in coalbeds: a new model. *Spe Reservoir Evaluation & Engineering*, **1**(6): 539-544.
- Parker, J., Lenhard, R. and Kuppusamy, T. 1987. A parametric model for constitutive properties governing multiphase flow in porous media. *Water Resources Research*, **23**(4): 618-624.
- Parkhurst, D. L. and Appelo, C. A. J. 1999. User's guide to PHREEQC (Version 2) : a computer program for

speciation, batch-reaction, one-dimensional transport, and inverse geochemical calculations. Water-Resources Investigations Report 99-4259, USGS.

Peng, D.-Y. and Robinson, D. B. 1976. A new two-constant equation of state. *Industrial and Engineering Chemistry Fundamentals*, **15**(1): 59-64.

Philip, Z. G., Jennings, J. W., Olson, J. E., Laubach, S. E. and Holder, J. 2005. Modeling coupled fracture-matrix fluid flow in geomechanically simulated fracture networks. *Spe Reservoir Evaluation & Engineering*, **8**(4): 300-309.

Pini, R., Storti, G. and Mazzotti, M. 2011. A model for enhanced coal bed methane recovery aimed at carbon dioxide storage. *Adsorption-Journal of the International Adsorption Society*, **17**(5): 889-900.

Poling, B. E., Prausnitz, J. M. and O'connell, J. P. 2001. *The properties of gases and liquids*, Mcgraw-hill New York.

Ray, C., Ellsworth, T. R., Valocchi, A. J. and Boast, C. W. 1997. An improved dual porosity model for chemical transport in macroporous soils. *Journal of Hydrology*, **193**(1-4): 270-292.

Robertson, E. P. 2005. Modeling Permeability in Coal Using Sorption-Induced Strain Data. SPE Annual Technical Conference and Exhibition. S. o. P. Engineers. Dallas, Texas.

Robertson, E. P. and Christiansen, R. L. 2008. A permeability model for coal and other fractured, sorptive-elastic media. *SPE Journal*, **13**(3): 314-324.

Ruthven, D. M. 1984. *Principles of adsorption and adsorption processes*. New York, Wiley.

Samardzioska, T. and Popov, V. 2005. Numerical comparison of the equivalent continuum, non-homogeneous and dual porosity models for flow and transport in fractured porous media. *Advances in Water Resources*, **28**(3): 235-255.

Schwartz, R. C., Juo, A. S. R. and McInnes, K. J. 2000. Estimating parameters for a dual-porosity model to describe non-equilibrium, reactive transport in a fine-textured soil. *Journal of Hydrology*, **229**(3-4): 149-167.

Scott, V., Gilfillan, S., Markusson, N., Chalmers, H. and Haszeldine, R. S. 2013. Last chance for carbon capture and storage. *Nature Climate Change*, **3**(2): 105-111.

Sedighi, M., Thomas, H. R., Masum, S. A., Vardon, P. J., Nicholson, D. and Chen, Q., Eds. 2015. Geochemical Modelling of Hydrogen Gas Migration in Unsaturated Bentonite Buffer. Gas Generation and Migration in Deep Geological Radioactive Waste Repositories. London, Geological Society, Special Publications.

Sedighi, M., Thomas, H. R. and Vardon, P. J. 2016. Reactive Transport of Chemicals in Unsaturated Soils: Numerical Model Development and Verification. *Canadian Geotechnical Journal*, **53**(1): 162-172.

Seetharam, S. C., Thomas, H. R. and Cleall, P. J. 2007. Coupled thermo/hydro/chemical/mechanical model for unsaturated soils - numerical algorithm. *International Journal for Numerical Methods in Engineering*, **70**: 1480-1511.

Shi, J. Q. and Durucan, S. 2004. Drawdown induced changes in permeability of coalbeds: A new interpretation of the reservoir response to primary recovery. *Transport in Porous Media*, **56**(1): 1-16.

Shi, J. Q. and Durucan, S. 2005. Gas storage and flow in coalbed reservoirs: Implementation of a bidisperse pore model for gas diffusion in a coal matrix. *Spe Reservoir Evaluation & Engineering*, **8**(2): 169-175.

Šimuněk, J. and van Genuchten, M. T. 2008. Modeling nonequilibrium flow and transport processes using HYDRUS. *Vadose Zone Journal*, **7**(2): 782-797.

Singhal, B. B. S. and Gupta, R. P. 2010. Applied hydrogeology of fractured rocks. Dordrecht, The Netherlands, Springer.

Thararoop, P., Karpyn, Z. T. and Ertekin, T. 2012. Development of a multi-mechanistic, dual-porosity, dual-permeability, numerical flow model for coalbed methane reservoirs. *Journal of Natural Gas Science and Engineering*, **8**: 121-131.

Therrien, R. and Sudicky, E. A. 1996. Three-dimensional analysis of variably-saturated flow and solute transport in discretely-fractured porous media. *Journal of Contaminant Hydrology*, **23**(1-2): 1-44.

Thomas, H. R. and He, Y. 1998. Modelling the behaviour of unsaturated soil using an elasto-plastic constitutive relationship. *Géotechnique*, **48**(5): 589-603.

Thomas, H. R., Sedighi, M. and Vardon, P. J. 2012. Diffusive reactive transport of multicomponent chemicals under coupled thermal, hydraulic, chemical and mechanical conditions. *Geotechnical and Geological Engineering*, **30**(4): 841-857.

Tsang, Y. W. and Pruess, K. 1987. A Study of Thermally Induced Convection near a High-Level Nuclear Waste

- Repository in Partially Saturated Fractured Tuff. *Water Resources Research*, **23**(10): 1958-1966.
- van Genuchten, M. T. 1980. A closed-form equation for predicting the hydraulic conductivity of unsaturated soils. *Soil science society of America journal*, **44**(5): 892-898.
- Ward, C. R. 2002. Analysis and significance of mineral matter in coal seams. *International Journal of Coal Geology*, **50**(1-4): 135-168.
- Warren, J. E. and Root, P. J. 1963. The Behavior of Naturally Fractured Reservoirs. *Society of Petroleum Engineers Journal*, **3**(3): 245-255.
- Wei, Y. S. and Sadus, R. J. 2000. Equations of state for the calculation of fluid-phase equilibria. *Aiche Journal*, **46**(1): 169-196.
- Wu, Y., Liu, J. S., Elsworth, D., Chen, Z. W., Connell, L. and Pan, Z. J. 2010. Dual poroelastic response of a coal seam to CO₂ injection. *International Journal of Greenhouse Gas Control*, **4**(4): 668-678.
- Xu, T. F. and Pruess, K. 2001. Modeling multiphase non-isothermal fluid flow and reactive geochemical transport in variably saturated fractured rocks: 1. Methodology. *American Journal of Science*, **301**(1): 16-33.
- Xu, T. F., Sonnenthal, E., Spycher, N., Pruess, K., Brimhall, G. and Apps, J. 2001. Modeling multiphase non-isothermal fluid flow and reactive geochemical transport in variably saturated fractured rocks: 2. Applications to supergene copper enrichment and hydrothermal flows. *American Journal of Science*, **301**(1): 34-59.
- Zhang, L. and Fredlund, D. 2003. Characteristics of water retention curves for unsaturated fractured rocks. *Proceedings of the 2nd Asian Conference on Unsaturated Soils*, Osaka, Japan.
- Zheng, L. and Samper, J. 2015. Dual-continuum multicomponent reactive transport with nth-order solute transfer terms for structured porous media. *Computational Geosciences*, **19**(4): 709-726.

Tables

Table 1 Material parameters used for verification Test I.

Parameter	Value
Residual volumetric water content,	
Saturated volumetric water content,	
Hydraulic constant, (m^{-1})	
Hydraulic constant, $(-)$	
Intrinsic permeability, (m^2)	
Absolute viscosity of water, $(Pa\ s)$	
Absolute viscosity of gas, $(Pa\ s)$	
Density of liquid water, $(kg\ m^{-3})$	

Table 2 Material parameters used for verification Tests II-a and II-b (Pini, Storti et al. 2011).

Parameter	Value		
Initial porosity, (-)			
Initial permeability, (m^2)			
Sorption rate, (s^{-1})			
Poisson's ratio, (-)			
Young's modulus, (Pa)			
Confining pressure, (Pa)			
Coal density, (kg m^{-3})			
(-)			
	CH ₄	CO ₂	N ₂
Viscosity, (Pa s)			
(-)			
Langmuir capacity, (mol kg^{-1})			
Langmuir constant (sorp.), (Pa^{-1})			
Langmuir strain, (-)			
Langmuir constant (swell.), (Pa^{-1})			

Table 3 Material parameters used for verification Tests III-a, III-b and III-c.

Material parameter	Relationship / value		
Volumetric weighting factor, (-)			
Degree of water saturation, (-)			
Retardation factor, (-)			
Longitudinal dispersivity, (m)			
	Fracture	Matrix	
Porosity, (-)			
Hydraulic conductivity, (m s^{-1})			
Coeff. of mechanical dispersion, (m^2s^{-1})			
	Test III-a	Test III-b	Test III-c
Solute mass exchange rates, (s^{-1})			

Figures

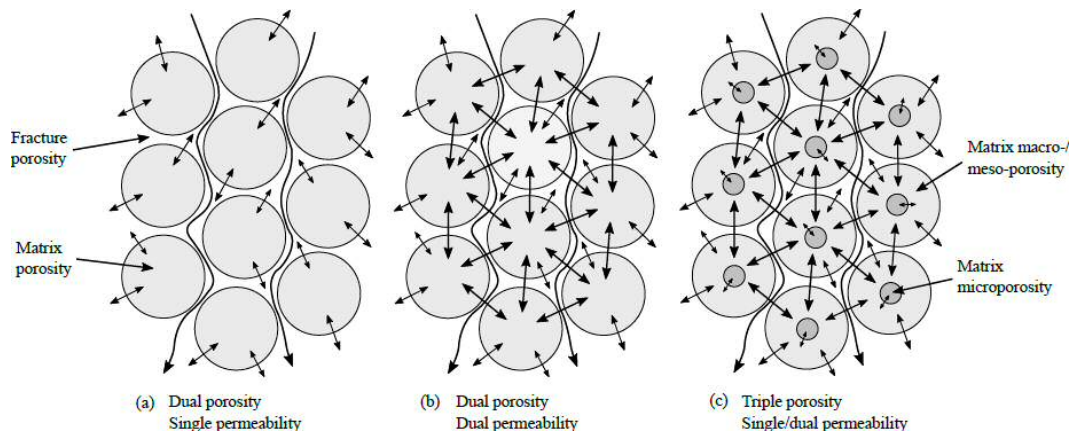


Figure 1 Illustration of the types of dual/triple porosity models (adopted and redrawn from Šimůnek and van Genuchten (2008)). Spheres represent the matrix porosity, including the partition of the macro- and micro-porosity where indicated. Gaps between the spheres represent the fracture porosity. Larger arrows denote permeability pathways and smaller arrows denote inter-porosity mass exchange.

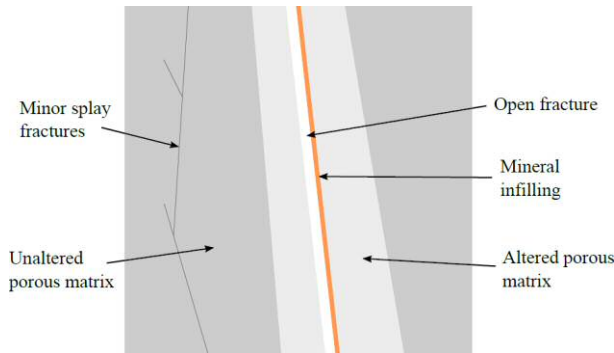


Figure 2 Schematic of a segment of a fractured rock, including open and minor fractures, mineral infillings, unaltered rock matrix, and altered rock matrix (adopted and redrawn from MacQuarrie and Mayer (2005)).

[COLOUR NOT REQUIRED IN FIGURE 2]

Upstream boundary conditions	Initial conditions	Downstream boundary conditions
$0 \leq t \leq 1 \text{ day}$ $Q_g = 0 \text{ mol s}^{-1}$ $1 \text{ day} \leq t \leq 11.6 \text{ days}$ Linear increase of Q_g to $1.0 \times 10^{-2} \text{ mol s}^{-1}$	$T = 298 \text{ K}$ $u_l = -1.8 \times 10^4 \text{ Pa}$ $u_g = RTc_g = 100 \text{ Pa}$	$u_l = 100 \text{ Pa}$ $u_g = RTc_g = 100 \text{ Pa}$ $\frac{\partial u_l}{\partial t} = RT \frac{\partial c_g}{\partial t} = 0.0$

Figure 3 Schematic of the initial and boundary conditions used for Test I.

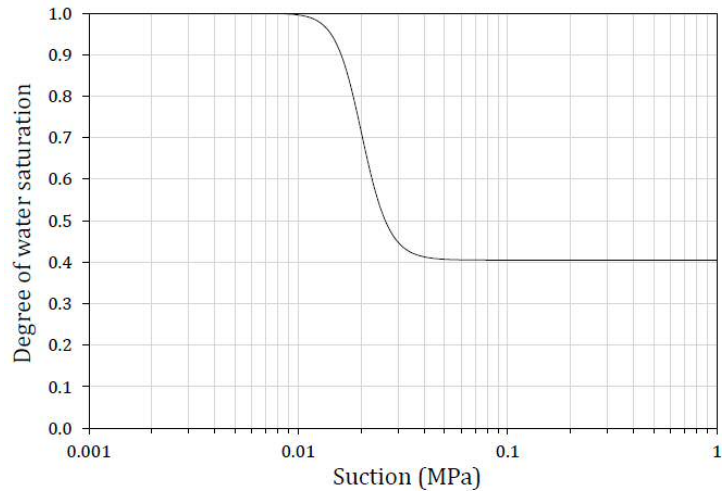


Figure 4 Water retention curve for Test I.

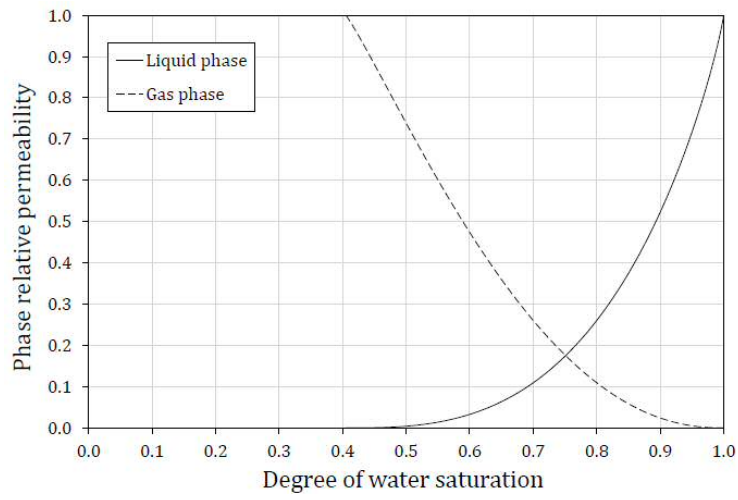


Figure 5 Phase relative permeability curves for Test I.

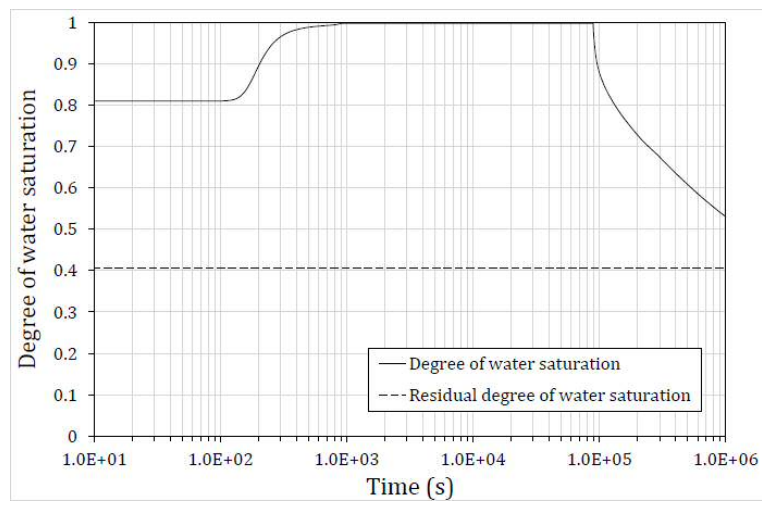


Figure 6 Predicted evolution of the degree of water saturation at the mid-point of the domain (m) for Test I.

Injection boundary conditions	Initial conditions	Production boundary conditions
<p>Test II-a:</p> $c_g^{CO_2} = 1,881.9 \text{ mol m}^{-3}$ <p>Test II-b:</p> $c_g^{N_2} = 1,522.5 \text{ mol m}^{-3}$	<p>Free gas (mol m^{-3}):</p> $c_g^{CO_2} = c_g^{N_2} = 0.0$ $c_g^{CH_4} = 582.4$ <p>Adsorbed gas (mol kg^{-1}):</p> $s_{gM}^{CO_2} = s_{gM}^{N_2} = 0.0$ $s_{gM}^{CH_4} = 0.75$	$RT \sum_{j=1}^{n_g} c_g^j$ $= 0.1 \times 10^6 \text{ Pa}$ $\sum_{j=1}^{n_g} \frac{\partial c_g^j}{\partial t} = 0.0$

Figure 7 Schematic of the initial and boundary conditions used for Test II-a (CO₂ injection) and Test II-b (N₂ injection).

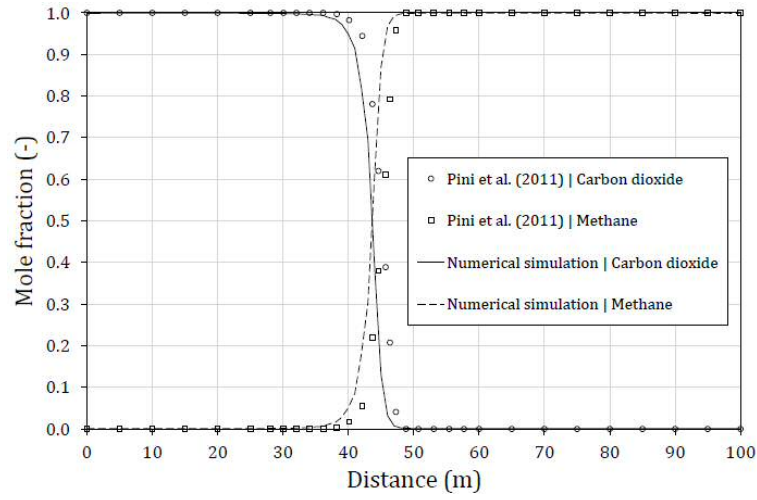


Figure 8 Gas composition of CO₂ and CH₄ (Test II-a) after 42 days compared to Pini et al. (2011).

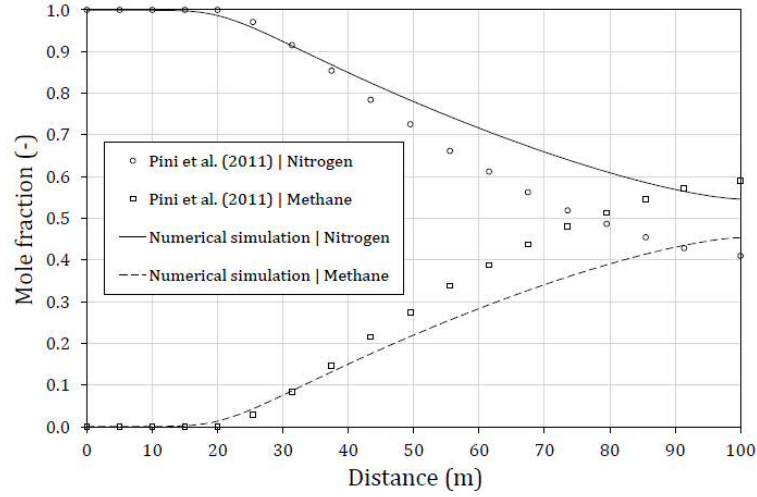


Figure 9 Gas composition of N₂ and CH₄ (Test II-b) after 42 days compared to Pini et al. (2011).

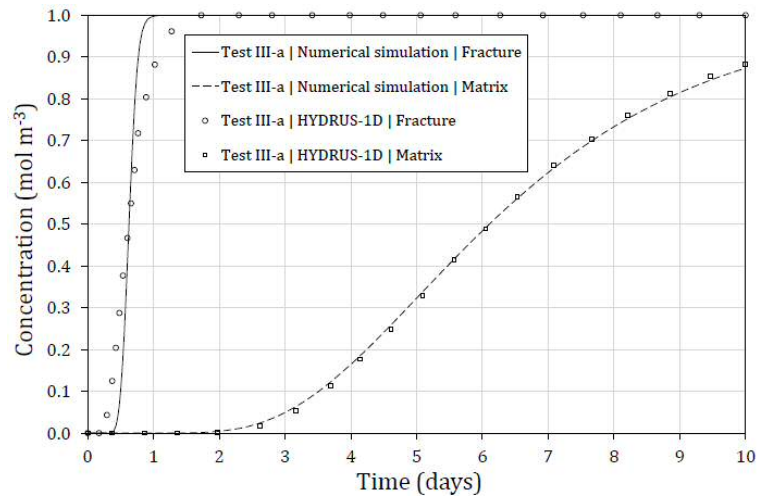


Figure 10 Chemical breakthrough for Test III-a (no mass exchange), obtained using the numerical model and by Šimunek and van Genuchten (2008) using HYDRUS-1D.

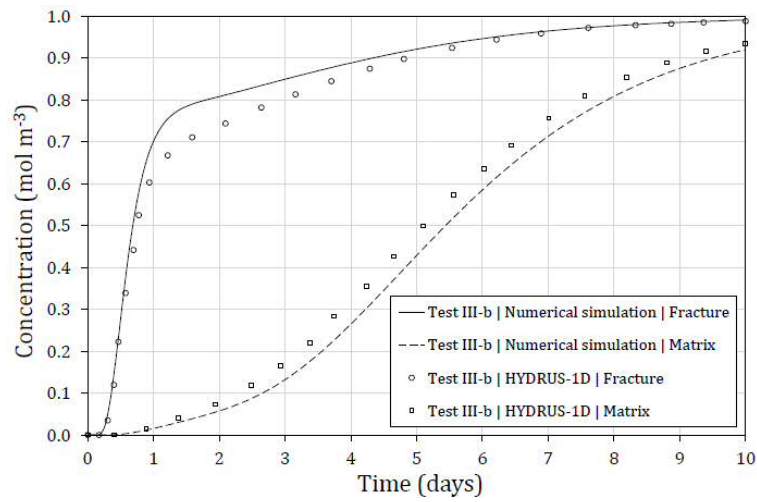


Figure 11 Chemical breakthrough for Test III-b (s-1), obtained using the numerical model and by Šimunek and van Genuchten (2008) using HYDRUS-1D.

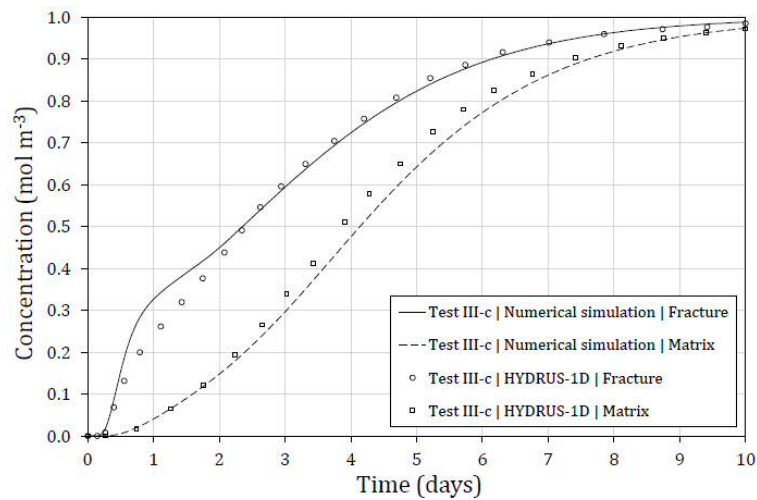


Figure 12 Chemical breakthrough for Test III-c (s-1), obtained using the numerical model and by Šimunek and van Genuchten (2008) using HYDRUS-1D.